ISSN: 2688-8645

Erosion Behavior and Surface Strengthening of Hydraulic Cylinders

Jianxu Hao [1, 2], Xingchang Zeng [1, 2, *], Gang Liao [1, 2], Tianzhou Li [3]

[1] National Engineering Research Center for Oil&Gas Drilling Equipment, Baoji Shaanxi, 721002, China

[2] Baoji Oilfield Machinery Co., Ltd, Baoji Shaanxi, 721002, China

[3] School of Mechatronic Engineering, Southwest Petroleum University, Chengdu Sichuan, 610500, China

* Corresponding author: Xingchang Zeng

Abstract

The tee is inevitably eroded by drilling fluid during operation, resulting in a decrease in its lifespan. The surface strengthening of the three-way inner cavity can effectively improve its service life. However, the specific erosion behavior and surface strengthening effect evaluation of the tee still need to be studied. This article establishes a computational model for the erosion behavior of the tee and the surface strengthening of the inner cavity through finite element simulation. The calculation results indicate that the maximum erosion rate occurs at the intersection line between the inlet and outlet straight pipes of the three-way joint. With the change of the operating conditions of the drilling fluid flow inlet and outlet, the maximum erosion position still occurs at the intersection line between the inlet and outlet straight pipes. After surface strengthening, the maximum deformation displacement of the three-way inner cavity can be effectively reduced by 33.93%, improving the impact resistance and service life of the three-way inner cavity.

Keywords

Tee Connection; Erosion Behavior; Surface Strengthening; Finite Element Simulation.

1. Introduction

The three-way valve, as an indispensable component of the drilling fluid circulation system, may encounter complex working conditions such as pressures of tens or even hundreds of megapascals, scouring by high-speed moving solid particles, and fluid corrosion, which makes it highly susceptible to erosion damage and prone to safety accidents [1-7]. Therefore, it is necessary to study the erosion behavior of the three-way valve to provide theoretical guidance for the strength and life evaluation of in-service manifold assemblies. Moreover, in order to increase the service life of the three-way valve, it is necessary to perform surface strengthening treatment on the inner cavity of the three-way valve, which will effectively prevent failure [8].

In response to the above issues, researchers both at home and abroad have conducted extensive studies. Yan Zhanghua [9] et al. based on the theory of fluid dynamics studied the erosion and wear mechanism of gravel movement on the high-pressure buckling pipe column, and obtained the influence laws of fluid helicity, tubing bending period, and particle characteristics on the erosion rate of the high-pressure buckling tubing. Xie Meng [10] et al. conducted erosion simulation modeling for the blind three-way junction between vertical and horizontal pipelines, analyzed the severely eroded positions within the blind three-way junction, as well as the influence of sand particle size and the length of the section with the plug on the ratio of the pipe

ISSN: 2688-8645

inner diameter (L/D) to the maximum erosion rate. Cui Lu [11] et al. based on the two-phase fluid model, carried out numerical simulation simulations according to different liquid phase displacements, inlet particle content, diameters and densities. Li Jinbao [12] et al. numerically simulated the anti-erosion and wear reduction capabilities of traditional 90° elbows and blind three-way junctions, providing theoretical guidance for the safe operation of gas transmission stations' gas distribution manifold. Zhu Xiaohua [13] et al. based on the two-phase flow particle erosion theory established a numerical calculation model for the erosion of the three-way junction, predicted the parts prone to erosion and wear during the use of the three-way junction, and studied the three-way junction orientation angle, the inlet flow rate of the fracturing fluid, the volume fraction of solid particles, the particle diameter and the density of the fracturing fluid on the erosion rate of the three-way junction. Lin Tiejun [14] et al. studied the motion trajectories of solid particles colliding with the substrate under a high-speed gas flow field, analyzed the erosion and wear laws of the gas-solid two-phase flow on the substrate surface at ultra-high speed. Zeng [15] et al. through the research on array electrode technology, completed the erosion behavior research on X65 carbon steel material bent pipes, and predicted the erosion and wear at different positions of the bent pipe on the CFD software.

Previous studies have obtained general rules for the erosion values of three-way fittings. However, the erosion laws under different installation and usage conditions of the three-way fittings, as well as how to reduce the erosion rate and increase the service life, are still not fully developed. With the rapid development of computer technology, numerical analysis methods have become a useful tool for evaluating erosion behavior and the effectiveness of surface strengthening [16-18]. Therefore, this paper uses the finite element analysis method to study the erosion behavior of three-way fittings under different usage conditions and the evaluation of the inner cavity surface strengthening.

2. The Erosion Behavior of the Three-Way Valve

2.1. Erosion Behavior Calculation Model

Triangular pipe fittings are widely used in the petroleum industry, mainly for guiding the diversion or convergence of fluid media within the pipe and changing the flow direction of the internal fluid media [19]. The tri-branch components cause significant disturbances to the fluid media in the process of diversion or convergence within the pipe, further promoting the friction and collision of the flowing media within the pipe and intensifying the formation of erosion phenomena. Therefore, the degree of erosion wear is more severe than that of straight pipes [20].

In this erosion analysis, the simulation calculation model adopts the k-ε turbulence model [21]. The inlet adopts a velocity inlet, and the inlet velocity is calculated based on the flow rate and inlet area. The outlet adopts an outflow boundary. There are many factors affecting erosion, and the erosion mechanism is relatively complex. It is mainly related to the physical properties and trajectories of particles, turbulence in the local flow field, solid wall conditions, the influence of multiphase flow, and the local cavities caused by material wear [22]. Therefore, there is no universal erosion model that can be applied to the simulation of all conditions. For different situations, different models should be selected. Fortunately, the forms of erosion models still have many similarities. The erosion rate is proportional to the particle diameter, particle velocity, collision angle, hardness of the solid surface, etc. The general form is as follows [2]:

$$-E_r \propto f(D_P) f(v) f(\alpha) f(H_S) \quad (1)$$

In the formula: E_r represents the erosion rate; D_p is the particle diameter; v is the particle velocity; α is the collision angle; H_s is the hardness of the solid surface.

This paper employs the Generic Erosion Model, and its general form is as follows [23]:

ISSN: 2688-8645

$$ER=\sum_{p=1}^{N_{trajct}}\frac{\dot{m_p}C(d_p)f(\alpha)v_p^n}{A_{face}} \quad (2)$$

In the formula: ER represents the erosion rate per unit area, in units of kg/$(m^2 \cdot s)$; m_p represents the mass flow rate of particles, in units of kg/s; $f(\alpha)$ is the collision angle function; v_p is the collision velocity of particles, in units of m/s, and n is the velocity exponent; $C(d_p)$ is the particle diameter function; A_{face} represents the area of the erosion region, in units of m^2.

During the solution calculation, the mass flow rate of the particles and the collision velocity are obtained through CFD calculations. The collision angle function is as shown in Equation (3) [9]:

$$f(\alpha)=\begin{Bmatrix}0.0, & \alpha=0°\\ 0.8, & \alpha=20°\\ 1.0, & \alpha=30°\\ 0.5, & \alpha=45°\\ 0.4, & \alpha=90°\end{Bmatrix} \quad (3)$$

In the formula: $f(\alpha)$ represents the collision angle function; α is the collision angle.

The collision speed and collision angle between the particles and the wall surface can be obtained from the particle trajectories. The erosion rate is generally closely related to the collision speed of the particles. It is generally believed that the erosion rate is proportional to the collision speed, and the erosion rate is the nth power of the collision speed. For steel, the value of n ranges from 1.5 to 2.7. In this paper, n is taken as 2.6 [24]. The particle size function $C(d_p)$=1.8e-9.

Figure 1a shows the geometric model of this paper, and the study is conducted on the three-way junction of the T-shaped structure as an example. Figure 1b shows one of the common working conditions, that is, a single inlet and double outlets. The blue marks represent the single inlet, and the red marks represent the double outlets. The calculation domain for the internal part of the three-way junction, that is, the erosion wear study, is drawn and meshed, and a high-quality structured hexahedral mesh is obtained [25]. The model after meshing is shown in Figure 1c. To further observe the meshing situation inside the three-way junction, Figure 1c is cut open, and the sectional view of the three-way junction cross-section is obtained, as shown in Figure 1d.

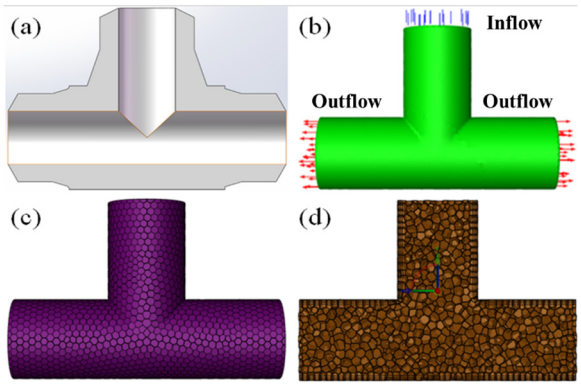

Figure 1. Three-way geometric model and erosion model (a) Geometric model, (b) Flow channel model diagram, (c) Element model diagram, (d) Middle section sectional view.

2.2. Flow Field Analysis

The working conditions for this analysis are as follows: the working pressure during the construction operation is 70 MPa, the flow rate Q is 55 L/s, and the selected drilling fluid is the typical drilling fluid from Chuanqing Drilling Company in Chuanne drilling. The density of the drilling fluid, ρ, is 1500 kg/m^3, the PV value is 20 MPa.s, and the particle diameter of the drilling

ISSN: 2688-8645

fluid is taken as the common 200 μm (75 mesh). The inlet boundary condition is a velocity inlet; the outlet is a free outflow. The pipe wall is a wall boundary, set as a stationary wall and a non-slip wall. The dispersed phase, namely the solid particles, is quartz stone particles. The escape condition is adopted at the inlet and outlet, the rebound condition is used for the wall, and transient numerical simulation is conducted for the two-phase flow in the three-way valve [26]. The diameter of the three-way valve inlet d is 101.6 mm, so the inflow velocity V of the drilling fluid in the three-way valve is:

$$V=\frac{Q}{\frac{\pi}{4}d^2}=\frac{0.055}{\frac{\pi}{4}\times 0.1016^2}=6.79\text{m/s} \quad (4)$$

The actual mass fraction of sand content in the drilling fluid, ω, is 0.3%, which meets the requirements of the DPM model for discrete phases. The DPM model is used to simulate the flow characteristics of the dilute dispersed phase in the flow field [27]. Then, based on the obtained actual mass fraction of sand content in the drilling fluid, the mass flow rate of the solid phase, P, in the liquid cylinder can be calculated as follows:

$$P = Q\omega\rho = 0.25kg/s \quad (5)$$

The flow field analysis was conducted under the conditions of an inlet velocity of 6.79 m/s and a mass flow rate P of 0.25 kg/s. The numerical results of the three-way flow field are shown in Figure 2. As can be seen from the velocity cloud diagram of the drilling fluid inside the three-way (Figure 2a), when the drilling fluid flows from the inlet into the straight pipe section, the velocity is relatively stable. When the drilling fluid flows from the inlet straight pipe section into the outlet straight pipe section, affected by the inertial force, the flow of the drilling fluid forms an arc and finally flows horizontally away from the inlet wall section. As can be seen from the trace and particle trajectory cloud diagrams inside the three-way (Figure 2b and c), the trace and particle trajectory are consistent with the velocity cloud diagram, especially near the intersection line, which indicates that the intersection line may suffer erosion damage.

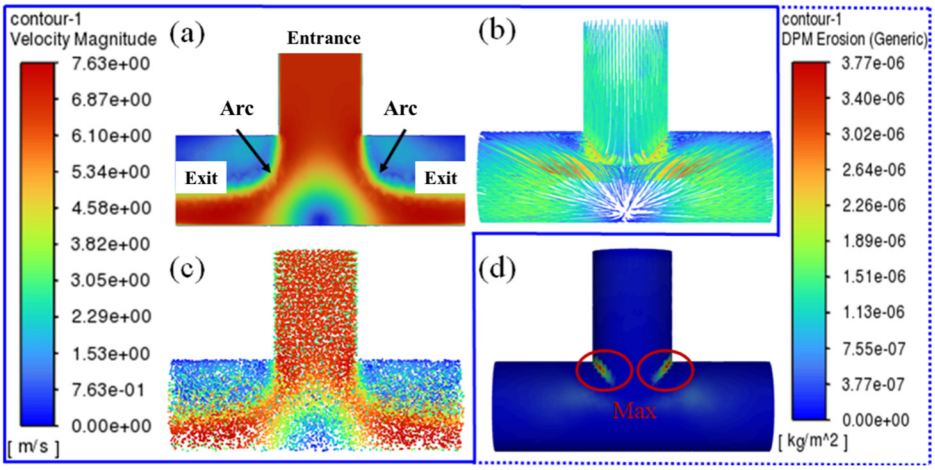

Figure 2. Analysis of three-way flow field (a) Velocity cloud map of drilling fluid inside the three-way, (b) Trajectory of drilling fluid inside the three-way, (c) Velocity cloud map of drilling fluid particles, (d) Overall erosion rate cloud map of the three-way.

To verify this conjecture, the overall erosion rate cloud diagram of the three-way was calculated, as shown in Figure 2d. From the overall erosion rate cloud diagram of the three-way, it can be seen that the erosion wear is mainly concentrated at the intersection line, and there is only a small amount of wear in the horizontal straight pipe section. This is similar to the previous experiments and simulations [1, 3, 9, 11], proving the accuracy of the numerical simulation in this paper. The fluid flows horizontally into the lower straight pipe section, and the fluid in the

ISSN: 2688-8645

upper straight pipe section flows vertically under the action of gravity. The two parts of fluid and particles collide at the intersection point of the two straight pipe sections, with chaotic motion trajectories and rebounding after hitting the wall. According to the velocity cloud diagram (Figure 2a and c), the velocity of the drilling fluid at the intersection line is high and the speed of the particles is fast, which has a strong ability to cause erosion damage to the wall. Therefore, the erosion wear at the intersection is relatively large. Most of the particles collide and continue to move with the fluid, and the impact angle on the wall in the straight pipe section is small, so the erosion wear in the straight pipe section is relatively small.

2.3. Analysis of Erosion Laws under Different Operating Conditions

Given that in actual operation, three-way valves may encounter various different working conditions, such as single inlet and single outlet, double inlet and single outlet, etc. Therefore, it is necessary to analyze these different working conditions and more comprehensively summarize the erosion patterns of three-way valves.

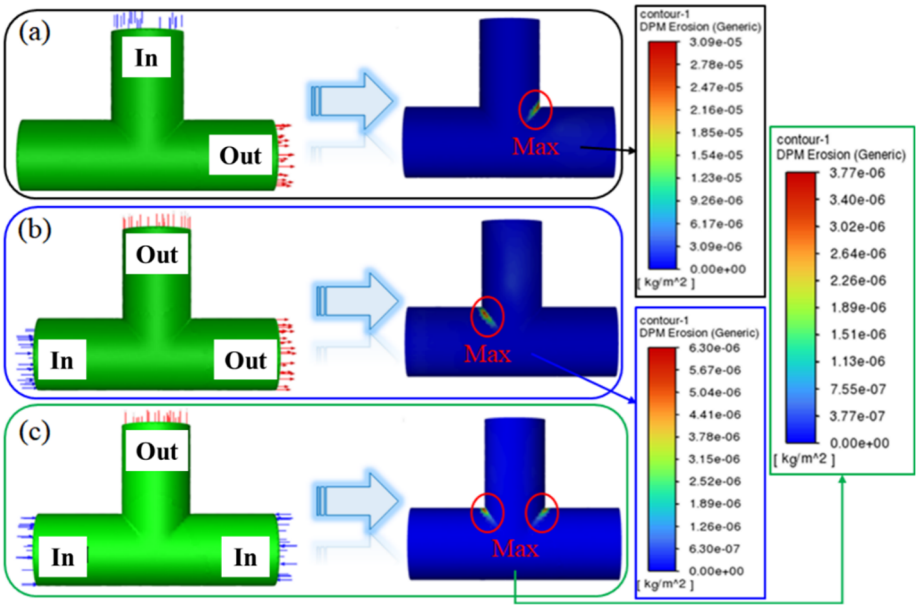

Figure 3. Erosion rate contour maps under different operating conditions (a) single inlet and single outlet, (b) single inlet and double outlets, (c) double inlet and single outlet

The flow field analysis was conducted under the condition of a mass flow rate P of 0.25 kg/s, as shown in Figure 3. The erosion rate contour maps for the single inlet single outlet, single inlet double outlet, and double inlet single outlet cases were calculated. From the erosion rate contour maps of the three-way different operating conditions, it can be seen that the maximum erosion position of the three-way always occurs on the intersection line of the inlet straight pipe and the outlet straight pipe. This may be because the fluid flows horizontally left and right in the lower straight pipe section, and the fluid in the upper straight pipe section flows vertically downward under the action of gravity. Then, the two parts of the fluid and particles may collide at the intersection line of the two straight pipe sections, causing the motion trajectory to become chaotic and complex. After hitting the wall near the intersection line, they continue to rebound. Therefore, the intersection line area suffers significant erosion wear. To further verify our speculation, the particle velocity contour maps under different operating conditions were studied, as shown in Figure 4. From the particle velocity contour map inside the three-way, it can be seen that in the intersection line of the inlet straight pipe and the outlet straight pipe in the three cases, the particle velocity is large, and the erosion angle at the intersection line is large. After hitting the wall near the intersection line, they continue to rebound. The

ISSN: 2688-8645

intersection line area experiences a large number of impacts, and the erosion damage caused by a single impact of the particle is strong, thus causing significant erosion wear at the intersection line area.

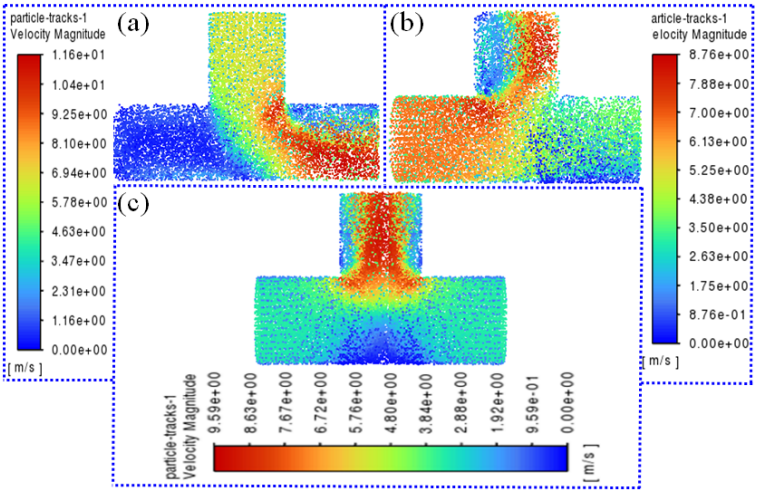

Figure 4. Particle velocity cloud diagrams under different operating conditions (a) single inlet and single outlet, (b) single inlet and double outlets, (c) double inlet and single outlet.

3. Surface Strengthening of the Inner Cavity of the Three-Way Valve

3.1. Computational Model for Surface Strengthening of the Inner Cavity

During operation, the inner cavity of the three-way valve also bears significant loads, which can cause deformation and damage to the cavity. Surface strengthening of the inner cavity can enhance its impact resistance and extend its service life. Therefore, it is necessary to conduct research on the surface strengthening of the three-way valve cavity. Currently, the three-way valve is mainly forged from 35CrMoA steel. The material properties of the three-way valve are shown in Table 1. Set the Young's modulus of 35CrMoA to 213 GPa (Group 1) as the control group, representing the situation without surface strengthening; other groups (Group 2, Group 3, Group 4) have Young's moduli set at 240 GPa and then increased by 320 GPa as a gradient for the experimental groups, representing the situation after surface strengthening measures are applied. Young's modulus can describe the ability of a solid to resist deformation. When the Young's modulus is larger, the probability of deformation is smaller [28]. After surface strengthening, the material's resistance to deformation may be enhanced [29]. Therefore, in this paper, the Young's modulus is set from 240 GPa to 320 GPa as a gradient for the experimental group to represent the material after surface strengthening, and to characterize the material after surface strengthening.

As shown in Figure 5, the finite element calculation model for the surface strengthening of the three-way cavity is presented. Figure 5a shows the result of the meshing. The meshing is carried out in a tetrahedral-dominated manner [30]. After the meshing is completed, the maximum cell size is 12mm, the number of nodes is 855,213, and the number of cells is 592,765. The boundary conditions are set according to the working conditions of the three-way, as follows:

(1) Set the gravitational acceleration in the vertical downward direction to g = 9.80 m/s^2;

(2) According to the installation method of the three-way, add full constraints to the inlet and outlet end faces of the three-way, with no degrees of freedom;

(3) Add symmetry constraints to the cutting surface of the three-way along the central axis of the cavity;

ISSN: 2688-8645

Table 1. Properties of the three-way material after surface strengthening treatment

35CrMoA (Group 1)			35CrMoA_1(Group 2)		
Density	7870	kg/m^3	Density	7870	kg/m^3
Young's modulus	213	GPa	Young's modulus	240	GPa
Poisson's ratio	0.286		Poisson's ratio	0.301	
Volume modulus	165.9	GPa	Volume modulus	201.0	GPa
Shear modulus	82.8	GPa	Shear modulus	92.2	GPa
35CrMoA_2(Group 3)			35CrMoA_3(Group 4)		
Density	7870	kg/m^3	Density	7870	kg/m^3
Young's modulus	280	GPa	Young's modulus	320	GPa
Poisson's ratio	0.314		Poisson's ratio	0.324	
Volume modulus	250.9	GPa	Volume modulus	303.0	GPa
Shear modulus	106.5	GPa	Shear modulus	120.9	GPa

(4) According to the working condition of the three-way, add a surface pressure of 70 MPa to the relevant surface (the red surface in Figure 5b).

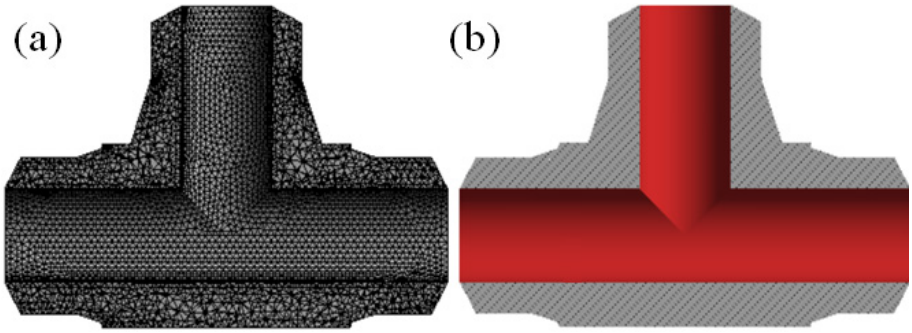

Figure 5. Mesh division and load application of the three-way junction (a) Mesh division result, (b) Load application surface

It is worth noting that, considering that the inner surface of the three-way connector is unstable in terms of surface pressure under the action of the drilling fluid in practice, a 70 MPa alternating load was applied to the inner cavity.

3.2. Evaluation of Inner Surface Strengthening

In order to evaluate the strengthening effect of the tricorner cavity, the deformation displacement of the tricorner was studied. Analyzing the magnitude of the deformation displacement can directly show how the surface strengthening effect is, and whether the deformation displacement of the cavity can be reduced to achieve the strengthening effect. In addition, through the analysis of the deformation displacement, the most severely deformed area of the tricorner deformation can be found, providing theoretical guidance for the actual

ISSN: 2688-8645

processing strengthening of the tricorner cavity surface. Based on the above discussion, the deformation displacement cloud diagrams of the tricorner cavities of different group numbers were visualized, as shown in Figure 6.

According to the results shown in Figure 6, the deformation displacement conditions of the tricorner cavities of different groups can be analyzed in greater depth. By comparison, it was found that the deformation displacement of group 1 was the largest, which might be caused by the insufficient structural design and material strength of this group to withstand the force situation. While the deformation displacement of group 2 was second, but still relatively large, which might also be related to the defects in the structural design and material strength. In contrast, the deformation displacements of group 3 and group 4 were relatively smaller, indicating that the structural design and material strength of these two tricorner groups were more reasonable and could better withstand the force situation.

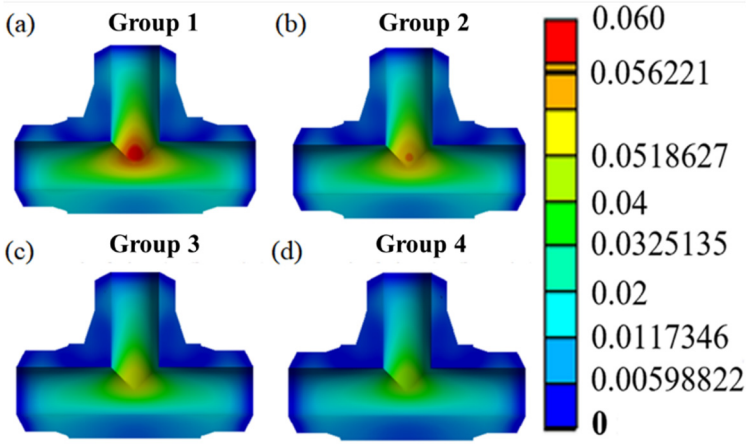

Figure 6. Deformation displacement cloud map of the inner cavity of the three-way valve.

It is worth noting that in all groups, the maximum deformation displacement seems to occur at the intersection line of the vertical pipe and the straight pipe, which is consistent with the previous research results [31]. This will well verify the accuracy of the finite element model in this paper. This phenomenon may be caused by the structure being too weak and prone to stress concentration at the intersection line. Therefore, in practical engineering applications, this area needs to be strengthened as a priority to improve the stability and strength of the structure. For example, secondary reinforcement can be appropriately considered in this area to further enhance the strength and stability of the three-way chamber cavity. Based on the above discussion, through surface strengthening treatment, the deformation displacement of the three-way chamber cavity has been effectively reduced, and the risk of material failure in the cavity has also been significantly reduced. In addition, during the analysis of the deformation displacement, it was found that the maximum deformation displacement area mainly concentrated at the intersection line of the vertical pipe and the straight pipe, which provides important theoretical guidance for actual strengthening processing.

To study the deformation displacement of the three-way chamber cavities in different group numbers more deeply, the trend of their maximum deformation displacements was calculated, as shown in Figure 7. From Figure 7, it can be seen that the maximum deformation displacement value of group 1 is the largest, reaching 0.056mm, while the maximum deformation displacement value of group 4 is the smallest, only 0.037mm. In contrast, the maximum deformation displacement values of group 2 and group 3 are 0.049mm and 0.042mm, respectively.

ISSN: 2688-8645

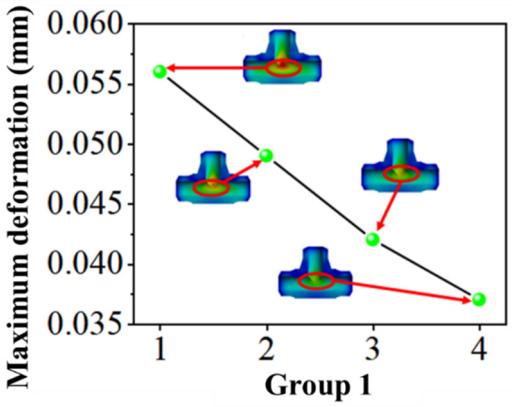

Figure 7. Maximum Deformation Displacement of the Three-way Junction.

Based on the analysis of the above data, the following conclusions can be drawn: Surface strengthening treatment can effectively reduce the maximum deformation displacement of the inner cavity of the three-way valve, thereby reducing the risk of significant deformation of the inner cavity and increasing the service life. Specifically, compared with the experimental group (Group No. 1), the maximum deformation displacement value of the three-way valve inner cavity after surface strengthening decreased by 33.93% (Group No. 4), which indicates that surface strengthening treatment is a very effective method that can significantly improve the stability and strength of the three-way valve inner cavity.

In conclusion, by calculating the maximum deformation displacement data of the three-way valve inner cavities of different group numbers, it has well proved the effectiveness of surface strengthening treatment, and further verified the previous conclusions. This research result will provide important guidance and reference for engineering practice, and is expected to promote the development of the strengthening processing technology of the three-way valve inner cavity.

4. Conclusion

This paper conducted finite element simulations to study the erosion behavior of the three-way valve and the evaluation of the internal cavity surface reinforcement.

(1) The analysis of the flow field of the drilling fluid inside the three-way valve indicated that the particle velocity was higher near the intersection line of the vertical pipe and the straight pipe, resulting in the maximum erosion rate occurring near the intersection line.

(2) By changing different working conditions, it was found that regardless of single inlet and single outlet, single inlet and double outlet, or double inlet and single outlet, the position where the maximum erosion rate occurred was always near the intersection line.

(3) Under the action of the internal cavity pressure, the maximum deformation displacement of the three-way valve also occurred at the intersection line of the vertical pipe and the straight pipe. After the internal cavity of the three-way valve was strengthened on the surface, it could effectively reduce the maximum deformation displacement, with a maximum reduction of 33.93%.

References

[1] ZHANG J X, BAI Y Q, KANG J, WU X. Failure analysis and erosion prediction of tee junction in fracturing operation[J]. Journal of Loss Prevention in the Process Industries, 2017, 46:94-107

[2] LI M Q, LIU F, ZHANG K, CHEN X, PENG H L. Advances in Liquid-solid Numerical Simulation of Pipeline Erosion[J]. Science Technology and Engineering, 2023, 23 (34):14497-14506.

[3] LI J B, MA C, LIU L J, LI X Q, et al. Numerical analysis of wear reduction characteristics of blind tee under sand-bearing gas flow erosion[J]. Natural Gas and Oil, 2022, 40(06):101-107.

[4] ZHUO K, QIU Y J, ZHANG Y D, WU D H. Analysis of the influence of particle parameters on erosion and wear of gas-solid two-phase flow[J]. Journal of Xi'an ShiYou University (Natural Science Edition), 2020, 35(06):100-106.

[5] XING L L, HUANG Z W, HU X Y. Fluid analysis of different types of three-way pipe joints based on ANSYS[J]. Science & Technology Information, 2021, 19(34):67-70.

[6] HUA J, ZHOU S Z, LI N. Finite element analysis and optimization of large four-way of 35MPa oil production wellhead device[J]. Journal of Oil and Gas Research, 2010, 32(02):154-156

[7] JIANG Y H, LI L F, ZHANG X Q. Analysis of four-way strength and improvement of flow channel structure of high-pressure large-bore wellhead[J]. China Equipment Engineering, 2022, (05):155-158.

[8] WANG J L, ZHOU T Z, FU L G, YU Y, LI C H. Effect of stress relief annealing on surface residual stress and microstructure properties of thick-walled tee of B10 copper-nickel alloy[J]. Metal Heat Treatment, 023, 48(07):111-116.

[9] LIAN Z H, WEI C X, SONG Z C, et al. Erosion damage mechanism of buckled tubing in high pressure and high production gas wells[J]. Oil Drilling and Production Technology, 2012, 34(01):6-9

[10] XIE M, LI X C, BAI W B, YU X, YANG H L. Numerical analysis of blind tee erosion in pneumatic conveying[J]. Mechanical Engineer, 2023, (04): 105-107.

[11] CUI L, HUANG S P, KANG W Q, et al. Study on erosion of multi-nozzle hydraulic jet tools under perforation condition[J]. Oil Drilling and Production Technology, 2018, 40(05):620-625.\

[12] LI J B, MA C, LIU L J, LI X Q. Numerical analysis of wear reduction characteristics of blind tee under sand-bearing gas flow erosion[J]. Gas & Oil, 2022, 40 (06): 101-107.

[13] ZHU X H, ZHANG Q, ZHANG Y M, DONG L L. Study on erosion and wear characteristics of high-pressure manifold tee[J]. surface technology, 2021, 50 (07): 258-265.

[14] LIN T J, LIAN Z H, CHENG S R, et al.Study on the drill pipe erosion of gas carrying cuttings in gas drilling[J]. Oil Drilling and Production Technology, 2010, 32(4): 1-4.

[15] ZENG L, ZHANG G A, GUO X P. Erosion-corrosion at different locations of X65 carbon steel elbow[J]. Corrosion science, 2014, 85(4): 318-330.

[16] MO L, LIU Q, XU X Y. Study on erosion and wear law of heterogeneous tee pipe based on CFD numerical simulation[J]. lubrication and Sealing, 2022, 47(08):41-46.

[17] MO L, FENG M, CHEN X, GUO Z X. Numerical simulation of erosion wear of elliptical disproportionate tee[J]. Surface Technology,2022,51(09):151-159.

[18] LIU H L,LI M Q,PAN L,JIANG Y X. Numerical simulation of the influence of T-shaped tee erosion under fracturing conditions[J]. Science Technology and Engineering,2020,20(10):3893-3897.

[19] CHEN Y,MA G Y. Numerical simulation of erosion and wear of liquid-solid two-phase flow in tee tube[J]. Mechanical Strength,2019,41(02):499-503.

[20] CHEN Y, MA G Y. Numerical simulation of the influence of connection structure size on erosion and wear of tee pipe[J]. China Safety Science and Technology, 2017, 13(12):91-97.

[21] ZHAO H Z, WANG J J, ZHOU S, ZHANG C, REN X Y, YANG C J. Spray cooling analysis of high-temperature produced gas for underground coal gasification based on DMP model and Realizable k-ε turbulence model[J]. Mechanical and Electrical Engineering Technology, 2023, 52(01):98-101.

[22] TAN H, YANG J, YE C Q, XIAO F, WANG W L, CAI R. Experimental study on erosion and wear of CT80 coiled tubing liquid-solid two-phase flow[J]. Petrole-um Tubing and Instruments,2023,52(01):98-101.

[23] Frawley P, Corish J, Niven A, et al. Combination of CFD and DOE to Analyse Solid Particle Erosion in Elbows[J]. International Journal of Computational Fluid Dynamics, 2009,23(5):411-426.

[24] HE P, LIANG Y R, AI X Y, HU Y Q, ZHANG C B, ZHANG D. Analysis of the influence of structural parameters on the erosion of eccentric reducers in gas/solid phase flow[J]. Journal of Xi'an Shiyou Universit-y (Natural Science Edition),2022,37(03):113-119

ISSN: 2688-8645

[25] WANG S, ZHU L Y, WANG Z B, HAN X. Numerical simulation of the influence of the length of the connecting pipe between elbows on the erosion of π-sha-ped pipe[J]. Oil & Gas Storage and Transportation, 2021, 40(11):1285-1292.

[26] CAO X W, LI X, ZHANG P, ZHANG W B, ZHANG Z G,BIAN J. Flow characteristics of annular flow in 90° horizontal elbow[J]. Oil & Gas Storage and Transportation, 2023,42(01):54-63.

[27] WANG Z L, WU Z H, WANG Z S, ZHANG M L, LIAO R Q. Simulation analysis of erosion of 90° curved flow channel in jet pump based on CFD-DPM[J]. Machine Tool and Hydraulics,2023,51(14):174-181.

[28] Roy A, Babuska T, Krick B, et al. Machine learned feature identification for predicting phase and Young's modulus of low-, medium-and high-entropy alloys[J]. Scripta Materialia, 2020, 185: 152-158.

[29] REN C X, WANG Q, HOU J P, ZHANG Z J, ZHANG Z F, LANGDON T G. The nature of the maximum microhardness and thickness of the gradient layer in surface-strengthened Cu-Al alloys[J]. Acta Materialia, 2021, 215: 117073.

[30] LIU T T,ZHENG P,LENG J L,LIU W J,XU Q,YANG Y. Local tetrahedral remeshing for adaptive computing[J]. Journal of Jilin University (Natural Science), 2021,59(06),1461-1468.

[31] XU H, WU W Y, WANG Z H,WANG Q L. Hydraulic characteristics analysis and flow field calculation of inclined tee pipes based on CFD[J]. Journal of Drainage and Irrigation Machinery Engineering, 2020, 38(11), 1138-1144.